Supporting Information

Co-immobilization of Enzymes and Cofactors Enabled by Liquid-Liquid Phase Separation for Continuous-Flow Catalysis

Chuyi Xiao,[a] Zhiyong Luo,[a] Yuyao Wan[a], Kaihui Xu,[a] Xingyuan Fang,[a] Dingyi Yang,[a] Ting Guo,[a] Hao Yuan[a], and Tao Meng [a,]*

[a.] School of Life Sciences and Engineering, Sichuan Engineering Research Center for Biomimetic Synthesis of Natural Drugs, Southwest Jiaotong University, Chengdu, Sichuan, 610031, PR China.

E-mail: taomeng@swjtu.edu.cn (T. Meng)

Supporting information contains the following details:

Number of pages: 21

Number of tables: 1

Number of figures: 12

Table of Contents

Experimental procedures；
Fig. S1, the effect of PEG&Dex concentration on the diffusion of NADH from the Dex to PEG phase;
Fig. S2, zeta potential of NADH, GDH, LDH and GLDH;
Fig. S3. The effect of PAH concentration (CPAH, wt%) on the diffusion (D, %) of NADPH or PLP from the Dex to PEG phase；
Fig. S4, partitioning behavior of PAH-50000 (a) and PAH-15000 (b) in 8 wt% PEG&Dex phases. (c) PAH-50000 (red bar) and PAH-15000 (blue bar) diffused (%) from Dex phase to PEG phase after 24 h and 100 h;
Fig. S5, zeta potential of Dex phase, 1 wt% PAH-loaded Dex phase and Zeta potential of 1 wt% PAH-loaded Dex phase after loading 1mM NADH;
Fig. S6, CD spectra of LDH before and after treatment with 8wt% Dex phase and 1 wt% PAH-loaded Dex phase;
Fig. S7. CLSM image of the FITC-GDH and Optical microscope image of RhoB at the interface of LLPS-CIS；
Fig. S8. Confocal laser scanning microscopy of the FITC-labeled GDH at the interface of LLPS, *t* = 0.5 and 60 min;
Fig. S9, Confocal laser scanning microscopy of the FITC at the interface of LLPS-CIS, *t* = 0.5 and 15 min.
Fig. S10. CLSM images of the water-in-oil (W/O) Pickering emulsion system stabilized by SiO_2 nanoparticles;
Fig. S11. The diffusion (*D*, %) of NADH and glucose from the Dex phase to the PEG phase in LLPS-CIS under different SSA conditions;
Fig. S12, The diffusion (D, %) of glucose from the PEG phase to the Dex phase in LLPS-CIS under different SSA conditions;
Table S1. the viscosity of 8 wt% PEG&Dex phases；
Table S2. Diffusion coefficient* of components in Dex phase or PEG phase；
Fig. S13. pictures of LLPS-CIS in reaction tubes with different size;
Fig. S14. enzyme activity retention rate of the LDH-GDH coupled reaction in the presence of the PAH;
Fig. S15. the effect of different concentration of ammonium sulfate (AS) on the diffusion of NADH from 1 wt% PAH-loaded Dex phase to PEG phase;
Table S3, comparison of literature data with this work;
Table S4. Structural formulas of the reactants involved in this study；
Supplementary references.

Experimental Procedures

1. Materials. Glucose dehydrogenase from *Bacillus sp.* (GDH, EC 1.4.1.2), pyruvic acid, α-ketoglutaric acid, poly (allylamine hydrochloride) (PAH, Mw = 15 kDa), oxidized nicotinamide adenine dinucleotide (NAD^+), and reduced nicotinamide adenine dinucleotide (NADH) were purchased from Aladdin (Shanghai, China). Glucose and rhodamine B isothiocyanate (RBITC) were purchased from Macklin (Shanghai, China). Poly (allylamine hydrochloride) (PAH, Mw = 50 kDa), Fluorescein Isothiocyanate (FITC), L-glutamate dehydrogenase from bovine liver (GLDH, EC 1.4.1.3), and L-lactate dehydrogenase from rabbit muscle (LDH, EC 1.1.1.27) were purchased from Sigma-Aldrich Chemical Corp. (St. Louis, USA). Dextran (Dex, Mw = 500 kDa) and polyethylene glycol (PEG, Mw = 8 kDa) were purchased from Spectrum Chemical Mfg. Corp., (California state, USA). Tris-HCl, ammonium chloride, Coomassie Brilliant Blue, dimethyl sulfoxide (DMSO) and NaOH were purchased from Kelong Chemical Reagents (Chengdu, China). All aqueous solutions were prepared with deionized (DI)water.

2. Preparation of the LLPS system. Polyethylene glycol/dextran (PEG/Dex) LLPS system (the following are abbreviated as LLPS system) were prepared by mixing PEG and Dex with Tris-HCl buffer (pH 7.4, 0.03 M), yielding final concentrations ranging from 6 wt% to 12 wt%. For instance, a PEG (6 wt%)/Dex (6 wt%) system was formed by dissolving 3 g of PEG and 3 g of dextran in 44 g of Tris-HCl buffer (0.03 M, pH 7.4). Similarly, a PEG (8 wt%)/Dex (8 wt%) system was prepared by dissolving 4 g of PEG and 4 g of dextran in 42 g of the buffer. LLPS system with final concentrations of 10 wt% and 12 wt% were prepared analogously. All systems were first stirred using an AKI magnetic stirrer (Tehtnica, Železniki, Slovenia) at 800 rpm, followed by standing until phase separation was visually observed and both phases became transparent. The viscosity of PEG&Dex phases, was measured with viscosimeter Brookfield-DV-C (Brookfield, USA).

3. Enzyme immobilization. Enzyme immobilization can be achieved through the partitioning effect and the macromolecular crowding effect of LLPS system. Briefly, enzyme was added to the obtained Dex phase (6, 8, 10 and 12 wt%) and mixed thoroughly with a final concentration of 0.5 or 1 mg/mL, then the separated PEG phase was carefully layered on top of the Dex phase to reform the biphasic system.

4. NADH immobilization. Prepared LLPS system was carefully separated into individual phases. To the obtained Dex-rich phase (Dex phase), the polyelectrolyte PAH (Mw 50,000 or Mw 15,000) was added and mixed thoroughly, achieving a final PAH concentration within the Dex phase ranging from 0.2 wt% to 2.0 wt%. Following PAH addition and mixing, the required amount of NADH (1 mM) was added to the Dex phase and mixed thoroughly. Subsequently, the separated PEG-rich phase (PEG Phase) was carefully layered on top of the modified Dex phase to reform the LLPS system.

5. Co-immobilization of enzyme and NADH. PAH was firstly added to the obtained Dex phase (8 wt%) and mixed thoroughly with a PAH concentration of 1 wt%, then enzymes and NADH

was added to the PAH-loaded Dex phase and mixed thoroughly, the separated PEG phase (8 wt%) was finally layered on top of the Dex phase to reform the biphasic system.

6. Quantification of the diffusion and partitioning of enzyme. To quantify the diffusion of the immobilized Enzyme, the Enzyme-loaded LLPS system (with 1 mM NADH initially in the Dex phase) was incubated for 24 or 100 h. The concentration of enzyme were determined using the Bradford method.[1] The diffusion of enzyme (D_E, %) was defined and calculated using the following formula:

$$D_E(\%) = \frac{[E]_{final} \times V_{PEG}}{[E]_{initial} \times V_{Dex}} \#(1)$$

Where the $[E]_{initial}$ (mg/mL) represents the concentration of enzyme initially added to the Dex phase, and the $[E]_{final}$ (mg/mL) denotes the concentration of enzyme measured in the PEG phase after incubating the biphasic system for 24 h or 100 h.

The partition coefficient (k) of enzyme was then calculated using the formula:

$$k_E = \frac{[E]_{PEG\ phase}}{[E]_{Dex\ phase}} \#(2)$$

7. Quantification of cofactor diffusion and partitioning. To quantify the diffusion of the immobilized cofactor, the NADH-loaded LLPS system (with 1 mM NADH initially in the Dex phase) was incubated for 24 or 100 h. Then the concentration of NADH in PEG phase was determined by a UV-1100 spectrophotometer (Mapada Instruments, Shanghai, China). The detection wavelength was set to 340 nm, corresponding to the characteristic absorption peak of NADH, where absorbance exhibits a linear relationship with concentration. Absorbance measurements were corrected for background interference from the blank solution where applicable.

The diffusion of NADH (D_{NADH}, %) was defined and calculated using the following formula:

$$D_{NADH}(\%) = \frac{[NADH]_{final} \times V_{PEG}}{[NADH]_{initial} \times V_{Dex}} \#(3)$$

Since the volumes of the PEG and Dex phases in the diffusion experiment were controlled to be identical, the formula can be simplified as follows:

$$D_{NADH}(\%) = \frac{[NADH]_{final}}{[NADH]_{initial}} \#(4)$$

Where the $[NADH]_{initial}$ (mM) represents the concentration of NADH initially added to the Dex phase, and the $[NADH]_{final}$ (mM) denotes the concentration of NADH measured in the PEG phase after incubating the biphasic system for 24 h or 100 h. The diffusion of NADPH and PLP was measured using the same method.

To investigate the partitioning behavior of NADH in the LLPS system, the system containing NADH was thoroughly homogenized by stirring into a single phase. Following re-equilibration and phase separation, the NADH concentration in each individual phase was quantified. The partition coefficient (*k*) was then calculated using the formula:

$$k_{NADH} = \frac{[NADH]_{PEG\ phase}}{[NADH]_{Dex\ phase}} \#(5)$$

8. Quantification of PAH diffusion and partitioning. The quantification method for the diffusion and partitioning of PAH was identical to that employed for NADH. However, the concentration of PAH was determined using a laboratory conductivity meter (Model MP513, Sanxin Instrument Factory). Specifically, the PEG phase containing PAH was diluted 25-fold with deionized water, and the conductivity of the diluted solution was subsequently measured. Calibration curves ($R^2 > 0.99$) correlating PAH concentration with conductivity were established using five-point concentration gradients spanning 0.1-1 wt%. Separate calibration curves were generated for each PAH molecular weight variant (Mw 50,000 and Mw 15,000).

9.Batch NADH Recycling Reactions. Batch reactions in the LLPS-CIS were conducted in the Reaction tubes. Generally, 0.2 mL of PEG phase, containing glucose (30 mM) and pyruvic acid (30 mM), was carefully layered on top of 0.2 mL PAH-loaded Dex phase, which contained NADH (1 mM), GDH (1 mg/mL) and LDH (0.5 mg/mL). The reaction was incubated at 37 °C for 1 h. Reaction conversion rates were calculated by periodically sampling and monitoring the substrate concentrations in the PEG phase. Taking glucose as an example, samples were mixed with a glucose assay kit purchased from Elabscience Biotechnology Co., Ltd. (Wuhan, China), incubated for 15 minutes, and then measured for absorbance using a spectrophotometer (UV-1100, Mapada Instruments). Glucose concentrations were subsequently determined by referring to a previously established standard curve. The Batch NADH Recycling reaction of GLDH and GDH was performed using the same method.

To vary the specific surficial area of the reaction, reaction tubes with different cross-sectional areas were used. In this study, three tubes with cross-sectional areas of 0.87 cm^2, 0.636 cm^2, and 0.384 cm^2 were employed. The specific surface areas (SSA, in this study, SSA is determined as the ratio of the interface area between the PEG phase and the Dex phase to the total volume of the Dex phase) was calculated by dividing the cross-sectional area by the volume of the Dex phase added to the reaction (0.2 mL).

10. Continuous-Flow NADH Recycling Reactions. Continuous-Flow NADH Recycling reactions in the LLPS-CIS were conducted in a custom-designed continuous-flow reactor with a volume of 1.95 mL. Generally, 0.8 mL 8 wt% Dex phase, which contained PAH (1 wt%), NADH (1 mM), GDH (1 mg/mL) and LDH (0.5 mg/mL), was loaded into the reactor, occupying its lower half as the stationary phase (with a specific surface area of 618.75 m^{-1} for the reaction). Subsequently, the 8 wt% PEG phase, containing glucose and pyruvic acid, (serving as the mobile phase) was introduced through one end of the upper half at different flow rates. The product was sampled and collected from the opposite end. Then, the conversion (%) and space-time yield (STY, g L^{-1} h^{-1}) were calculated following the equations:

$$Conversion\ (\%) = \frac{[S]_{inlet} - [S]_{outlet}}{[S]_{inlet}} \#(6)$$

$$STY\ (g\ L^{-1} h^{-1}) = \frac{[P]_{outlet} \times Q}{V_R} \#(7)$$

Where $[S]_{inlet}$ (mM) represents the substrate concentration at the inlet of the reactor tube, $[S]_{outlet}$ (mM) represents the substrate concentration at the reactor outlet, $[P]_{outlet}$ represents the product concentration at the reactor outlet, Q represents the flow rate, and V_R represents the effective volume of the reactor (for this specific reactor, V_R = total reactor volume − volume of loaded Dex phase).

To investigate the versatility of the system, a cofactor regeneration catalytic reaction coupling GLDH (0.5 mg/mL) and GDH (1 mg/mL) was also performed, converting α-ketoglutarate and NH_4^+ to glutamate.

11. Zeta Potential Measurement. Zeta potential of the Dex phase was measured with Zetasizer Nano ZEN3600 (Malvern, UK). Briefly, the prepared Dex phase with or without 1 wt% PAH (Mw 50,000 or Mw 15,000) was first diluted 5-fold with Tris-HCl buffer (0.03 M, pH 7.4) and then added to the zeta potential cuvette for three consecutive tests. Zeta potential of PAH-loaded Dex phase with NADH was also measured with the same method. Zeta potential of NADH was also measured with Zetasizer Nano ZEN3600. Briefly, 1 mM NADH solution containing 0.03 M Tris-HCl buffer (pH 7.4) was added to the zeta potential cuvette for three consecutive tests. Zeta potential of LDH, GDH and GLDH was also measured with Zetasizer Nano ZEN3600. Briefly, 0.5 mg/mL enzyme solution containing 0.03 M Tris-HCl buffer (pH 7.4) was added to the zeta potential cuvette for three consecutive tests.

12. Fluorescence labeling enzymes. To determine the enzymes and NADH loading within the Dex phase, the enzymes were labeled with different dyes. Fluorescein isothiocyanate (FITC) or rhodamine B isothiocyanate (RhoB) labeling enzymes were synthesized according to the methods reported previously. [2] In brief, 0.2 mL of 5 mg/mL FITC dimethyl sulfoxide solution was added dropwise to 2 mL of PBS (0.05 M, pH 7.0) containing GDH (5 mg/mL). Stir the mixture at 25°C for 4 hours. Terminate the reaction by adding 2 mL of 50 mM NH_4Cl aqueous solution. Finally, the FITC-labeled GDH were obtained through ultrafiltration by a centrifugal

filter (MWCO 3.5-5 kDa) several times until no fluorescence in the filtrate. RhoB-labeled LDH was prepared using the same method.

13. CLSM Characterization. 10 μL of the FITC-labeled GDH solution and 10 μL of the RhoB-labeled LDH solution were mixed into 200 μL of the Dex phase. Subsequently, 0.8 μL of the mixed solution was dispensed into the PEG phase to form microdroplets for observation. A confocal laser scanning microscopy (A1, Nikon, Japan) was then used to observe the droplets loaded with different dye-labeled enzymes and NADH. Observations were made 2 minutes after microdroplet formation.

14. Circular Dichroism (CD) spectroscopy. The CD spectra were measured with the CD spectrometer (J-1500, Jasco, Japan). The continuous scanning of CD spectra was carried out with a data pitch of 0.1 nm, response time of 1.0 s, and bandwidth of 1.0 nm at a scanning speed of 100 nm min^{-1}. To explore the effects of dextran and PAH on protein secondary structure, the CD spectra of the enzymes alone were tested over the wavelength range of 190-250 nm. 1 mL solution of 0.03 M Tris-HCl buffer (pH 7.4) containing 1 mg of enzyme, 80 mg dextran (8 wt%), and 10 mg PAH (1 wt%) was prepared and incubated for 24 hours. This solution was then diluted 5-fold with 0.03 M Tris-HCl buffer (pH 7.4), transferred to a quartz cell (1.0 mm path length), and was scanned under the same wavelength range. The solution without PAH and the solution without both PAH and dextran were scanned using the same method. Note that all obtained spectra were scanned three times, and the background was subtracted.

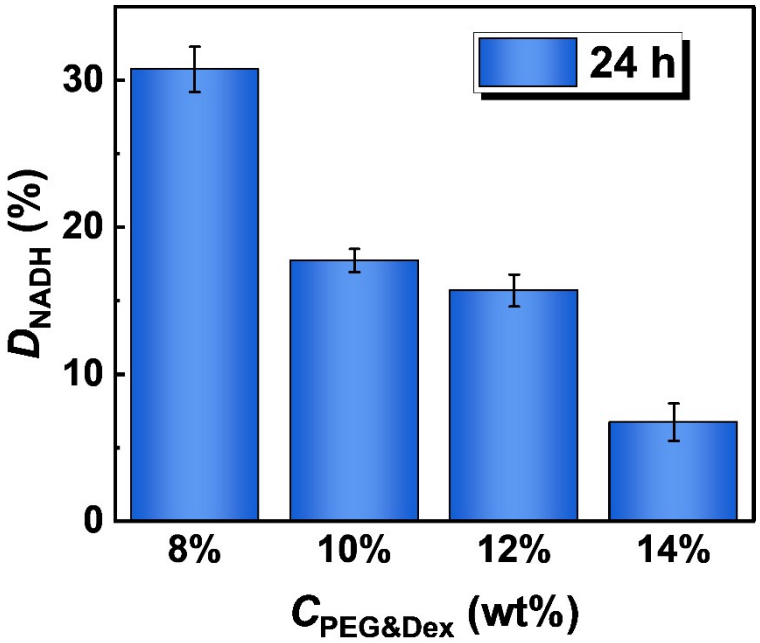

Fig. S1. The effect of PEG&Dex concentration (C_{PAH}, wt%) on the diffusion (D, %) of NADH from the Dex to PEG phase in LLPS.

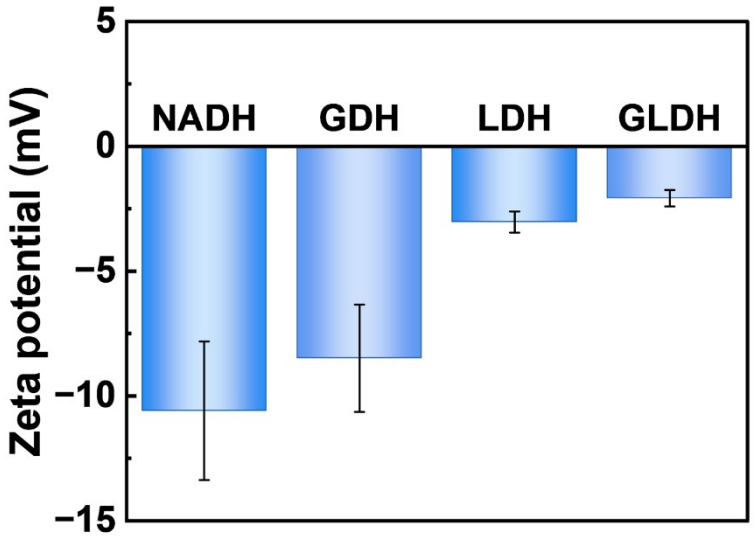

Fig. S2. Zeta potential of NADH, GDH, LDH and GLDH in Tris-HCl buffer (0.03 M, pH 7.4).

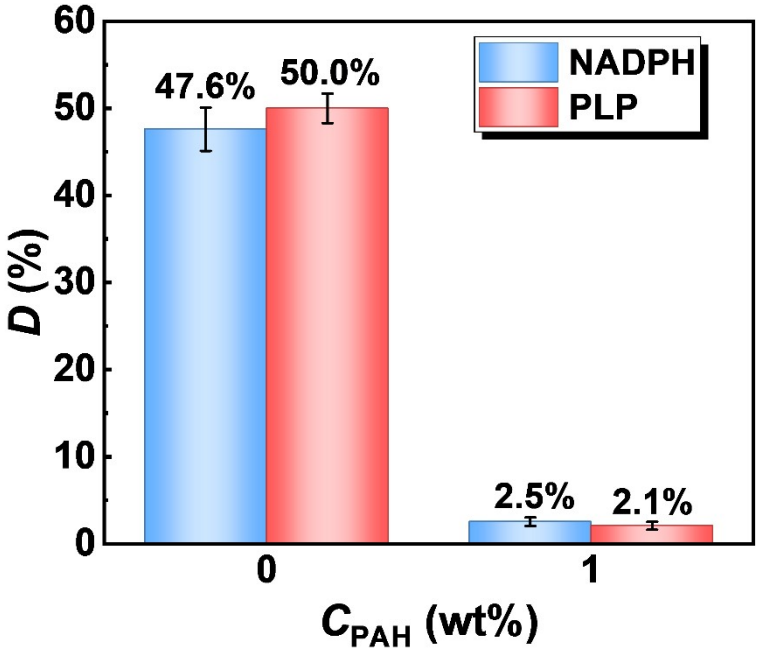

Fig. S3. The effect of PAH concentration (C_{PAH}, wt%) on the diffusion (D, %) of NADPH or PLP from the Dex to PEG phase, t = 100 h.

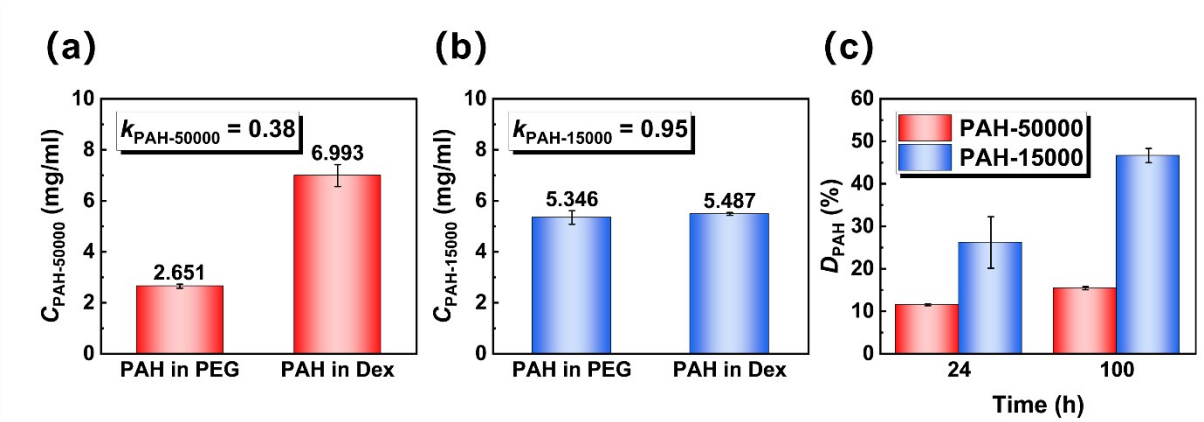

Fig. S4. (a-b) Partitioning behavior of PAH-50000 (a) and PAH-15000 (b) in 8 wt% PEG&Dex phases. (c) PAH-50000 (red bar) and PAH-15000 (blue bar) diffused (*D*, %) from Dex phase to PEG phase after 24 h and 100 h.

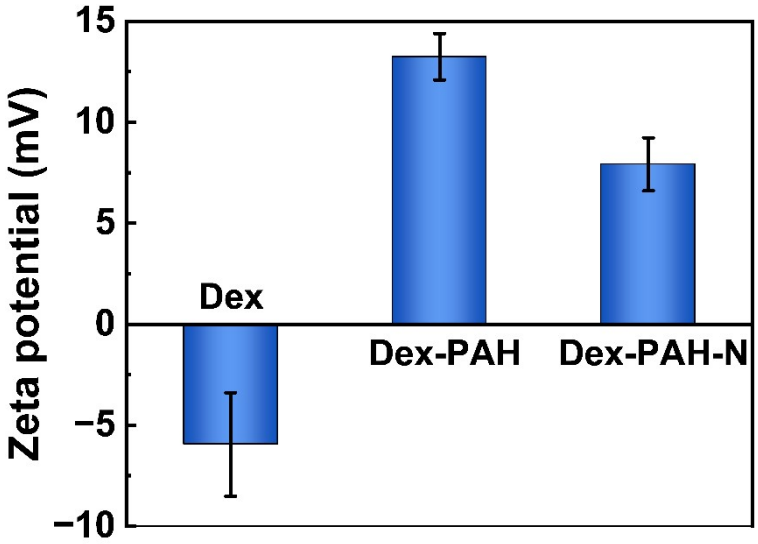

Fig. S5. Zeta potential of Dex phase (8 wt%), 1 wt% PAH-loaded Dex phase and Zeta potential of 1 wt% PAH-loaded Dex phase after loading 1mM NADH.

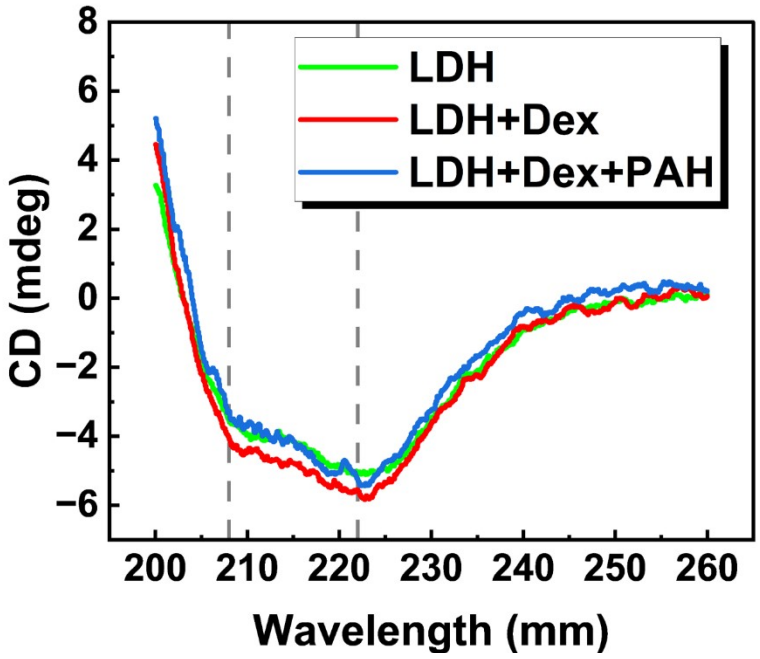

Fig. S6. CD spectra of LDH before and after treatment with 8wt% Dex phase and 1 wt% PAH-loaded Dex phase.

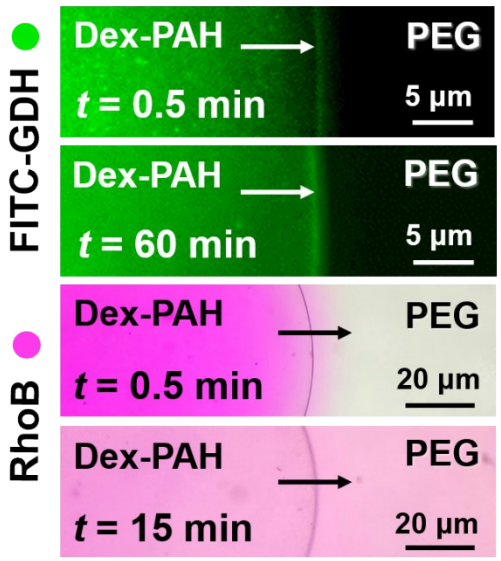

Fig. S7. CLSM image of the FITC-GDH (*t* = 0.5 and 60 min) and Optical microscope image of RhoB (*t* = 0.5 and 15 min) at the interface of LLPS-CIS.

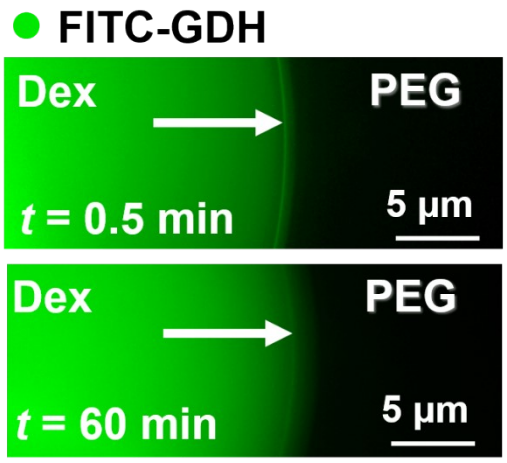

Fig. S8. Confocal laser scanning microscopy of the FITC-labeled GDH at the interface of LLPS, *t* = 0.5 and 60 min.

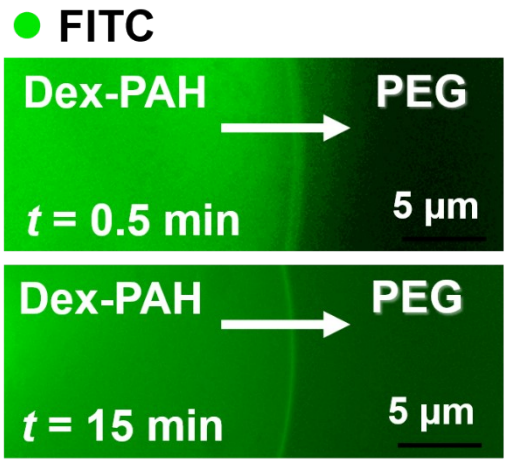

Fig. S9. Confocal laser scanning microscopy of the FITC at the interface of LLPS-CIS, *t* = 0.5 and 15 min.

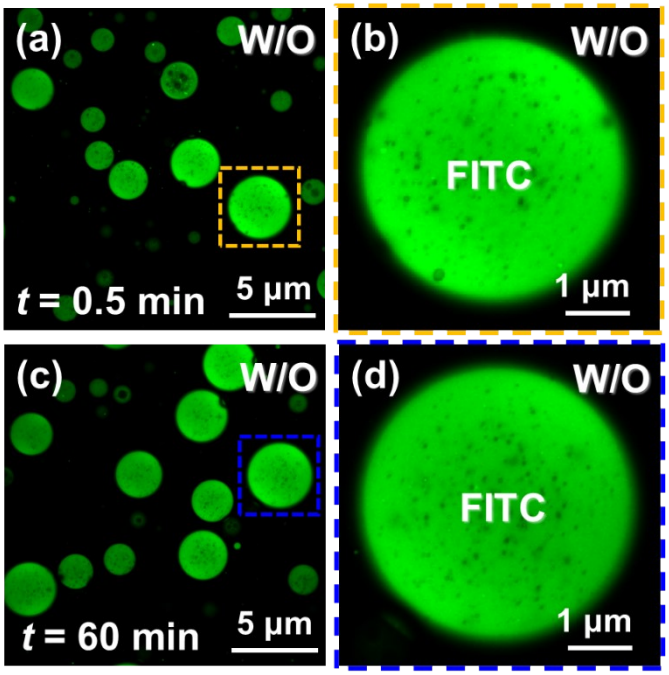

Fig. S10. CLSM images of the water-in-oil (W/O) Pickering emulsion system stabilized by SiO_2 nanoparticles. (a-b) images with FITC in the aqueous phase acquired at t = 0.5 min; (c-d) images with FITC in the aqueous phase acquired at t = 60 min.

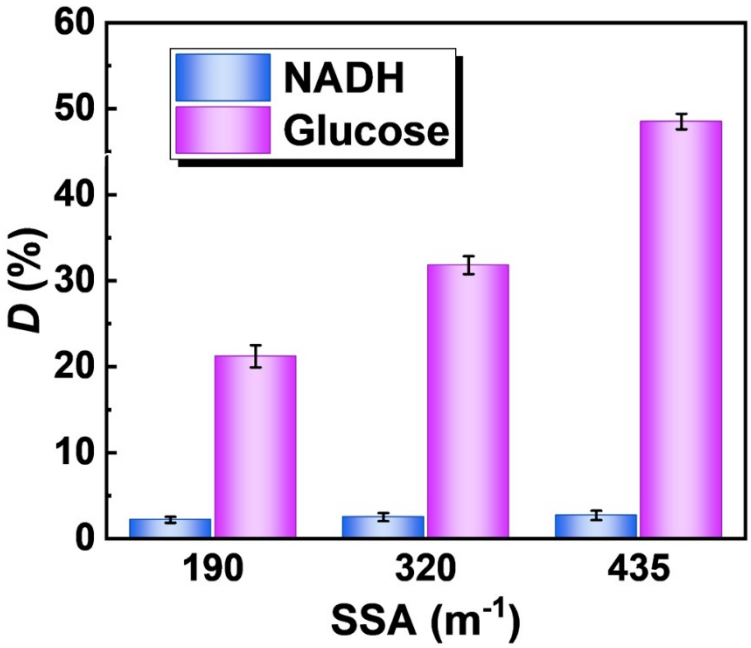

Fig. S11. The diffusion (*D*, %) of NADH and glucose from the Dex phase to the PEG phase in LLPS-CIS under different SSA conditions (for NADH, *t* = 24 h; for glucose, *t* = 60 min).

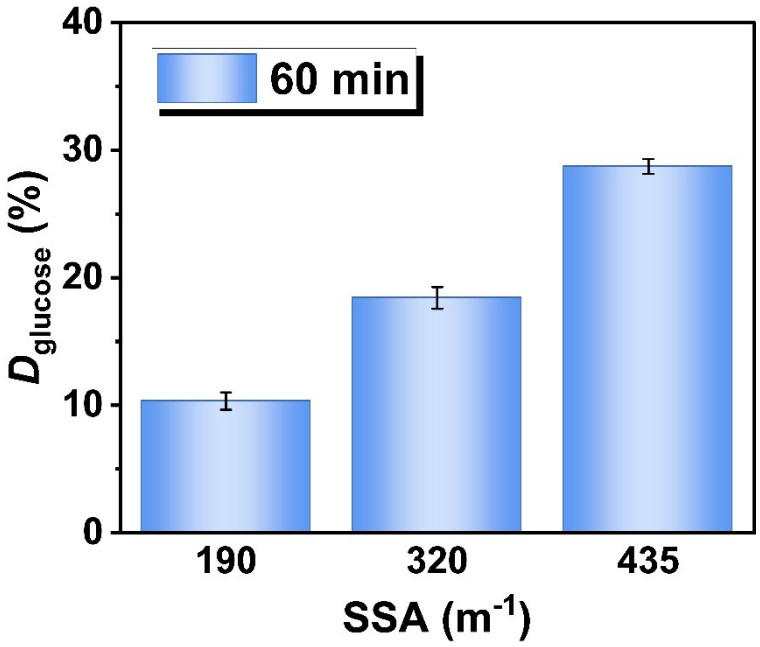

Fig. S12. The diffusion (*D*, %) of glucose from the PEG phase to the Dex phase in LLPS-CIS under different SSA conditions *t* = 1 h.

Table S1. the viscosity (η) of 8 wt% PEG&Dex phases

Phases	viscosity (cP)
Dex phase	313.0
PEG phase	5.8

Table S2. Diffusion coefficient* of components in Dex phase (d_{Dex}) or PEG phase (d_{PEG})

Components	d_{Dex} (m^2/s)	d_{PEG} (m^2/s)
Glucose	2.15×10^{-12}	1.15×10^{-10}
Pyruvic acid	1.99×10^{-12}	1.07×10^{-10}
NADH	5.58×10^{-13}	2.98×10^{-11}

*The diffusion coefficient (d) of enzyme was then calculated using the formula:

$$d = \frac{kT}{6\pi\eta R}$$

where k is the Boltzmann constant with a value of 1.38×10^{-23} J/K, T is the temperature (298 K), η is the solution viscosity, and R is the radius of the species.

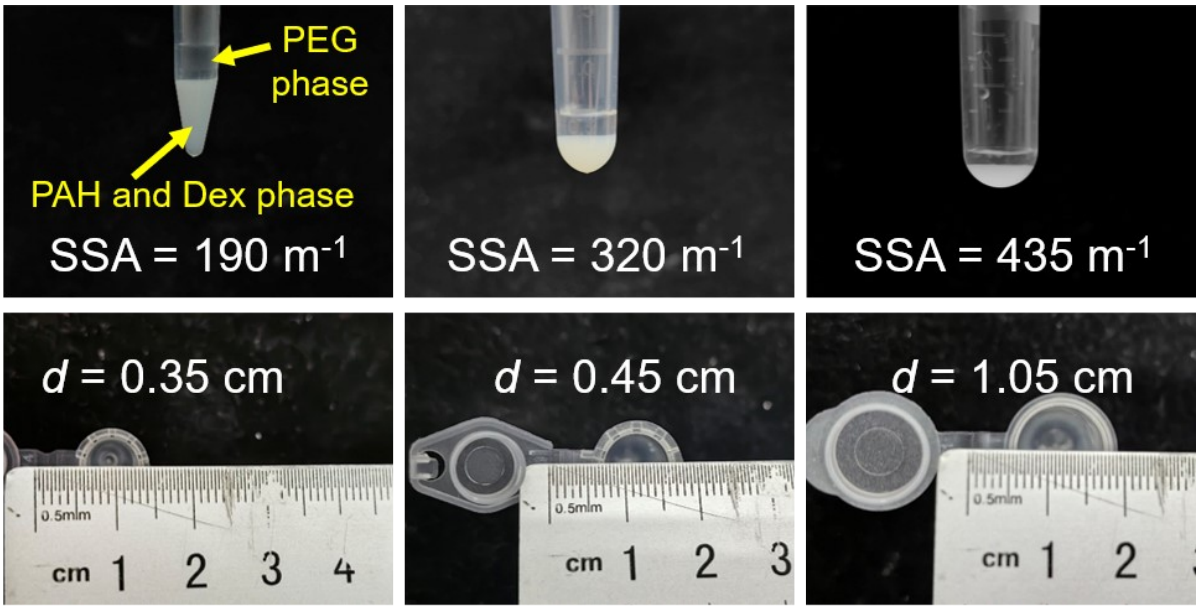

Fig. S13. Pictures of LLPS-CIS in reaction tubes with different size, the transparent upper phase is PEG phase, the lower phase is PAH-loaded Dex phase, due to the different diameters of the reaction tubes, systems with different specific surface areas (SSA, m^{-1}) can be obtained.

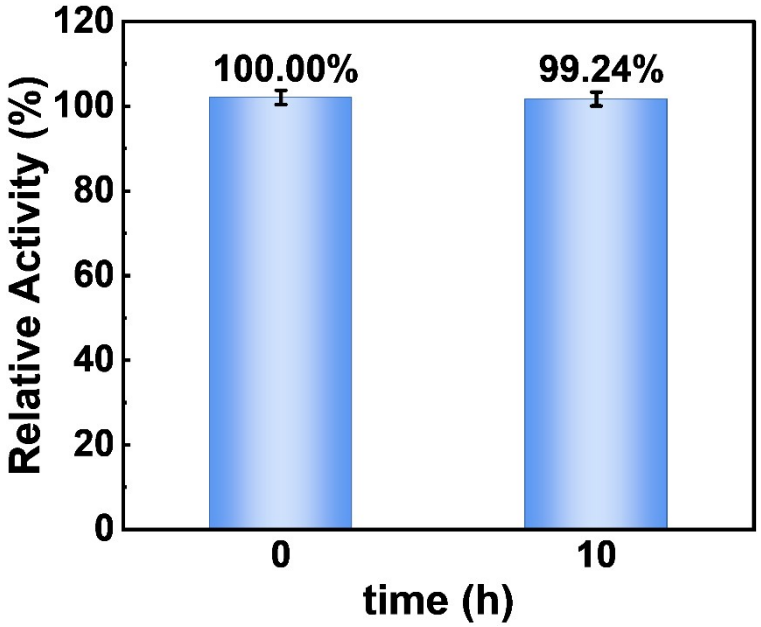

Fig. S14. enzyme activity retention rate of the LDH-GDH coupled reaction in the presence of the PAH at *t* = 0 h or *t* = 10 h.

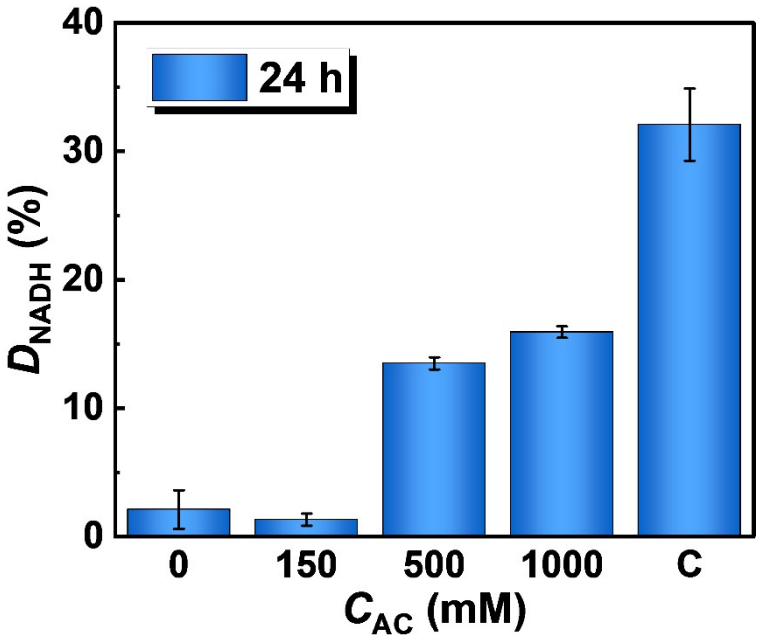

Fig. S15. The effect of different concentration (0, 150, 500 and 1000) of ammonium chloride (AC, NH_4Cl) on the diffusion of NADH in LLPS-CIS from Dex phase to PEG phase. C: the diffusion of NADH from pure Dex phase (8 wt%) to PEG phase (8 wt%).

Table S3. Comparison of literature data with this work*

Ref	cofactor	Flow rate ($mL \cdot min^{-1}$)	Conversion (%)	$V_{reactor}$ (mL)	Time (h)	TTN
This work	NADH	0.017	87-70	1.15	10	1505
Angew. 2017[3]	NADH	0.05	99-79	0.25	107	85
ACS SCE. 2023[4]	NADH	0.025	99	0.25	21	20
Angew. 2023[5]**	NADPH	0.017	90	5.4	300	59204
G. C. 2024[6]	NADH	0.05	81-49	1.4	50	2984
ACS SCE. 2024[7]	NADH	0.01	87-73	1.5	2.5	34

*The listed literature focused on the co-immobilization systems of multienzyme and phosphorylated cofactors for continuous-flow biocatalysis.

**This system is based on water-in-oil Pickering emulsions, a design that fails to catalyze hydrophilic substrates.

Table S4. Structural formulas of the reactants involved in this study

Reactants	Structure
Glucose	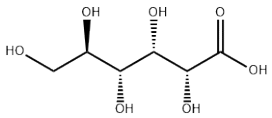
Glucose acid	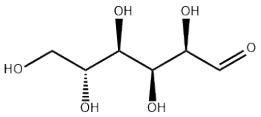
Pyruvic acid	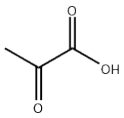
L-lactate	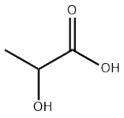
α-Ketoglutaricacid (AKG)	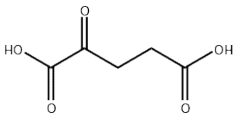
Glutamate	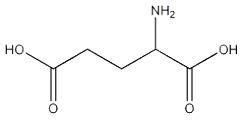
NADH	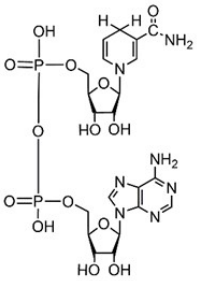
NAD^+	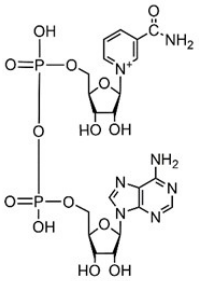

Supplementary References

1. M. M. Bradford, *Anal. Biochem.*, 1976, 72, 248−254.
2. S. Liu and Y. Sun, *Angew. Chem., Int. Edit.*, 2023, 62, e202308562.
3. S. Velasco-Lozano, A. I. Benítez-Mateos and F. López-Gallego, *Angew. Chem., Int. Edit.*, 2017, 56, 771−775.
4. E. Diamanti, S. Velasco-Lozano, D. Grajales-Hernández, A. H. Orrego, D. Di Silvio, J. M. Fraile and F. López-Gallego, *ACS Sustain. Chem. Eng.*, 2023, 11, 14409−14421.
5. W. Wei, R. Ettelaie, X. M. Zhang, M. Fan, Y. Dong, Z. B. Li and H. Q. Yang, *Angew. Chem, Int. Edit.*, 2022, 134, e202211912.
6. D. Andrés-Sanz, A. Maiz-Iginitz, J. M. Bolivar, A. H. Orrego, H. Sardon and F. López-Gallego, *Green Chem.*, 2024, 26, 4563−4573.
7. J. Santiago-Arcos, S. Velasco-Lozano, E. Diamanti, A. I. Benítez-Mateos, D. Grajales-Hernández, F. Paradisi and F. López-Gallego, *ACS Sustain. Chem. Eng.*, 2024, 12, 9474−9489.